LBL-13347
Preprint

Lawrence Berkeley Laboratory

UNIVERSITY OF CALIFORNIA

RECEIVED
LAWRENCE
BERKELEY LABORATORY
NOV 13 1981
LIBRARY AND
DOCUMENTS SECTION

Materials & Molecular Research Division

Submitted to the Journal of Chemical Physics

THE ANGULAR AND VELOCITY DISTRIBUTIONS OF NO SCATTERED FROM THE Pt(111) CRYSTAL SURFACE

W.L. Guthrie, T.-H. Lin, S.T. Ceyer, and G.A. Somorjai

August 1981

TWO-WEEK LOAN COPY

This is a Library Circulating Copy which may be borrowed for two weeks. For a personal retention copy, call Tech. Info. Division, Ext. 6782

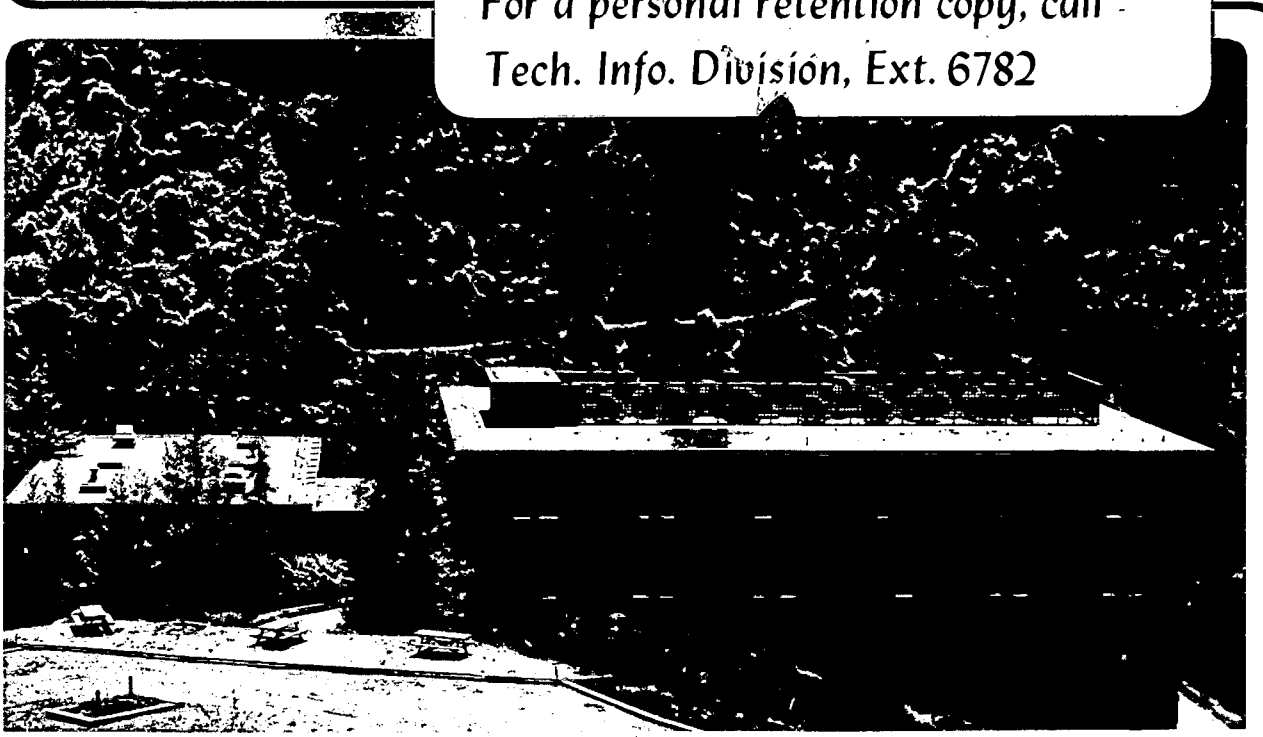

LBL-13347

Prepared for the U.S. Department of Energy under Contract W-7405-ENG-48

DISCLAIMER

This document was prepared as an account of work sponsored by the United States Government. While this document is believed to contain correct information, neither the United States Government nor any agency thereof, nor the Regents of the University of California, nor any of their employees, makes any warranty, express or implied, or assumes any legal responsibility for the accuracy, completeness, or usefulness of any information, apparatus, product, or process disclosed, or represents that its use would not infringe privately owned rights. Reference herein to any specific commercial product, process, or service by its trade name, trademark, manufacturer, or otherwise, does not necessarily constitute or imply its endorsement, recommendation, or favoring by the United States Government or any agency thereof, or the Regents of the University of California. The views and opinions of authors expressed herein do not necessarily state or reflect those of the United States Government or any agency thereof or the Regents of the University of California.

THE ANGULAR AND VELOCITY DISTRIBUTIONS OF NO SCATTERED FROM THE Pt(111) CRYSTAL SURFACE

W.L. Guthrie, T.-H. Lin, S.T. Ceyer*, and G.A. Somorjai

Materials and Molecular Research Division, Lawrence Berkeley Laboratory,
and
Department of Chemistry, University of California, Berkeley, CA 94720

Abstract

The angular and velocity distributions of NO scattered from the Pt(111) surface have been studied in the temperature range of 475 K - 1200 K. Three different kinetic energy nozzle beams were used. Both angular and velocity distributions confirm the coexistence of inelastic and trapping-desorption scattering processes. Trapping probability decreases as incident beam energy increases, indicating that the adsorption is not activated. For beams with a kinetic energy of $\langle KE \rangle/2k$ equal to 265 K and 615 K, the trapped molecules were found to be equilibrated with the surface for T_s between 475 K and 900 K.

.....

*Present Address: National Bureau of Standards
Washington, DC 20545

This work was supported by the Director, Office of Energy Research, Office of Basic Energy Sciences, Materials Sciences Division of the U.S. Department of Energy under Contract W-7405-ENG-48, and the National Science Foundation.

Introduction

The molecular beam-surface scattering experiment is well suited to explore the magnitude and the nature of energy transfer between the incident gas atoms or molecules and the surface. In the past, most of the energy exchange information was obtained by monitoring the angular distribution of scattered molecules [1,2]. Recently, however, velocity distributions and energy distribution in internal rotational and vibrational states have been measured for the incident and scattered beams in various laboratories [3-9]. Ultimately, one would like to determine the angular, velocity and internal energy state distributions for the same molecular beam-surface system to be able to fully describe the gas-surface interaction.

We have developed instrumentation to measure the velocity distribution of both incident and scattered molecules from single crystal surfaces under ultra-high vacuum conditions. Using supersonic or atomic beams we can determine the angular distribution of the scattered moelcules and the velocity distribution at each angle of scattering.

In this paper we report the velocity and angular distributions of nitric oxide, NO, scattered from a Pt(111) single crystal surface. We chose NO because its high sticking probability (0.7-0.8) and high heat of adsorption ($\Delta H \simeq 29$ kcal/mole, without substantial dissociation to its atomic constituents that makes strong energy transfer very probable [11,12]. In addition, several groups [8-10] measured the internal energy state distribution of NO after surface scattering by laser induced fluorescence. Three different kinetic energy nozzle beams were used in our experiments to determine how the incident beam velocity influences the energy transfer process.

Experimental

A schematic diagram of the molecular beam-surface scattering aparatus is shown in Figure 1. While this instrument has been described in detail elsewhere [13,14], a brief review of its essential features is appropriate here. The two incident beams could originate from either 0.003" diameter nozzle or 0.039" diameter effusion sources, depending on the experimental requirements. For NO scattering from the platinum crystal surface, only one nozzle source is used with the pressure behind the nozzle of 200 torr. The scattering chamber, which is pumped by a noble ion pump, a titanium sublimator, and a liquid nitrogen trapped diffusion pump, is equippped with instruments for Auger electron spectroscopy (AES), low energy electron diffraction (LEED), ion sputtering of the crystal surface, and the crystal manipulator. The sample is heated by electron bombardment, and a Pt-Pt 10% Rh thermocouple is used to monitor its temperature, T_s. The background pressure in the scattering chamber is in the 10^{-10} torr range.

The two-stage differentially pumped detector chamber, which is enclosed in the scattering chamber, is rotatable about sample at the center of the scattering chamber. A quadrupole mass spectrometer in the detector chamber is used for signal analysis. A pseudo-random slit chopper, which is mounted on the detector chamber, is used for time-of-flight analysis. Since the scattered beam is chopped instead of the incident beam, the time-of-flight distributions are not affected by unknown surface residence times. The flight path from the chopper to the mass spectrometer ionizer is about 12 cm. To obtain the angular scattering distribution, 150 hz tuning fork chopper is used to modulate the incident beam.

Note that the mass spectrometer is density sensitive rather than flux sensitive. Thus to calculate the flux mean kinetic energy and the spread of the velocity distributions, we calculated the velocity moments M_1, M_2, and M_3

from the time-of-flight data. The moments, M_I (I=1,2,3) are defined as follows:

$$M_I = \int_0^\infty v^I P(v)dv \qquad (1)$$

where P(v)is the density velocity distribution of the scattered molecules in the detector. M_1 is proportional to the flux into the detector. The flux mean kinetic energy, <KE>, and the spread of the velocity distribution, $\langle\sigma^2\rangle$, are given by

$$\langle KE\rangle = (1/2)m\langle v^2\rangle = (1/2)m\ M_3/M_1 \qquad (2)$$

$$\langle\sigma^2\rangle = (\langle v^2\rangle-\langle v^2\rangle)/\langle v\rangle^2 = M_1M_3/M^2 - 1 \qquad (3)$$

where m is the mass of the molecule. For a beam with a Maxwellian density distribution at temperature T, the flux mean kinetic energy will be 2kT instead of (3/2)kT and $\langle\sigma^2\rangle$ will be 0.132. Hereafter the term "a beam energy T K" will mean that the beam mean kinetic energy is equal to 2kT.

In our experiments, NO supersonic beams by three different flux mean kinetic energies <KE>/2k=265, 615, and 1390 K were used. The corresponding $\langle\sigma^2\rangle$ are 0.026, 0.038, and 0.024, respectively. Beams of 265 and 1390 K were obtained by anti-seeding NO with xenon and seeding with helium while keeping the nozzle at room temperature. A TOF distribution for one of the direct beams is shown in Fig.2.

The single crystal Pt(111) was cleaned with argon ion sputtering, oxygen treatment, and annealing. The cleanliness was checked by AES before and after the experiment. In all of our experiments, the angle of incidence was ~ 51°. TOF was taken by moving the detector either to 7° from the surface normal or to specular and the surface temperature (T_s) was varied from 475 K to 1195 K. The pseudo-random chopper was operated at 180 hz. It took 15 to 25 minutes to obtain each TOF distribution depending on the incident beam energy.

After some of the NO scattering experiments, AES showed slight oxygen contamination for crystal temperatures below 900 K and minor calcium and oxygen contamination for crystal temperatures above 1000 K. The typical oxygen surface concentration was about .1 monolayer, and the calcium contamination was about .05 monolayer.

To check how the small amount of Ca and O contamination might affect the results, we carried out the scattering experiment in the presence of different amounts of oxygen and calcium on the platinum surface in the coverage range of zero to about 0.5 monolayer. We did not find any clear difference in TOF distribution. Thus the energy transfer does not appear to be affected by the presence of small concentrations of low weight atoms of oxygen and calcium.

Since the commercially available nitric oxide purity is only 99%, there is some possibility that the oxygen contamination is from NO_2 impurity [15]. To check this possibility, we purified NO gas by distillation from a LN_2/n-pentane slush at 113 K into a LN_2 trap, but found not clear change in the level of the oxygen contamination when using 99.98% or 99% NO beams. It appears that a very small amount of NO does dissociate on the Pt(111) surface during scattering and is the source of the surface oxygen.

The angular distribution of scattered helium beams was found to be sensitive to the surface roughness and cleanliness [16]. In order to determine the structural roughness of our Pt(111) single crystal sample, we scattered helium beams when pure and when mixed with NO. For pure helium scattering, the full width at half-maximum (FWHM) is below 2°, while the resolution of the detector is 1.5°. For the helium seeded mixture, all FWHM of the reflected helium beams are about 1.5°, for T_s varied from 475 K to 1110 K. These narrow angular distribution are indicative of clean and flat surfaces.

A TOF distribution of NO from an effusive source at 300 K is shown in Fig. 3. The solid curve is the corresponding Maxwellian distribution at 300 K. As one can see, the agreement between the theoretical curve and the data points from the effusive source is excellent. Several TOF distributions of effusive thermal beams were taken in order to calibrate the flight path and also the zero flight time channel.

Results

Typical time-of-flight distributions for NO scattered from the (111) crystal face of platinum under different experimental conditions are displayed in Figs. 4 and 5. The experimental variables are the crystal temperature, T_s, the incident beam energy, and the detection angle, either specular or near the surface normal. All the solid curves corespond to the Maxwellian distributions at the respective crystal temperature. Although the average energies for Figs. 4a and 4b are about equal, 505 K and 487 K, respectively, their $\langle\sigma^2\rangle$ values are different since Fig. 4b has a sharper peak than Fig. 4a. Fig. 5a and 5b are examples of the lack of equlibration of scattered NO with the platinum crystal surface.

We have taken about 100 spectra at various experimental conditions. Instead of presenting the complete body of data, we present the two important parameters of the TOF distribution, the average flux mean kinetic energy in units of K, and the velocity spread, $\langle\sigma^2\rangle=(\langle v^2\rangle-\langle v\rangle^2)/\langle v\rangle^2$, as a function of the different experimental variables. In Figures 6,7, and 8, these parameters are plotted as a function of crystal temperature for the three different NO incident beam velocities.

The incident beam energy for the data of Fig.6 is 1390 K. From Fig. 6a

it is clear that for T_s<900 K the scattered beam energy at the specular scattering angle is larger than that at the surface normal, and both are different from the surface temperature. For T_s>900 K, the scattered beam energies at both specular and normal angles are similar to the surface temperature. However, the identity of the scattered beam kinetic energy with the surface temperature does not imply equilibration with the surface as can be seen from Fig. 6b. The $\langle\sigma^2\rangle$ are too small in the specular direction compared with that of a Maxwellian distribution. Fig. 5b clearly shows that the scattered beam distribution is narrower than a Maxwellian distribution at the specular angle. An important feature of Fig. 6b is that $\langle\sigma^2\rangle$ for the normal detection have the value of the Maxwellian distribution, while $\langle\sigma^2\rangle$ for the specular detection are all smaller than 0.132 and decrease at T_s increases.

The incident beam kinetic energy for the data of Fig. 7 is 615 K. At the surface normal the kinetic energy of the scattered NO beam is equal to T_s for T_s<900 K, and becomes smaller than T_s above 900 K. In the specular direction, the scattered beam kinetic energy shows the same trend and in general it has less kinetic energy than at the surface normal, especially at high surface temperatures. Fig. 7b shows that $\langle\sigma^2\rangle$ in the specular direction is smaller than near the surface normal at low T_s, but $\langle\sigma^2\rangle$ at the two scattering angles become almost equal at high T_s. The difference in the widths of the distributions at low surface temperature is visually evident in Fig.4.

The incident beam energy for the data of Fig. 8 is 265 K. The scattered beam energy shows the same trend as a function of T_s as that shown in Fig. 7a. In general, the scattered beams in Fig. 8 have less kinetic energy than the corresponding beams in Fig. 7a at high T_s for both specular and normal scattering. For T_s below 800 K, the scattered beams' kinetic energies at normal are independent

of incident beam energies, 265 K vs. 615 K, and equal to the corresponding surface temperatures; $\langle\sigma^2\rangle$ of the scattered beams for this incident beam energy, 265 K, are not shown because of large errors due to the weaker signal.

The angular distributions for different surface temperatures and incident beam energies are shown in Fig.s 9, 10, and 11. Since the mass spectrometer detects particle density and not flux, the data in these figures are angular density distributions. The important features of the angular distribution are as follows: For a fixed incident beam energy, the degree of specularity increases as the surface temperature increases. For a fixed T_s, the degree of specularity increases as the incident beam energy increases.

Discussion

We find that NO scattered from the platinum (111) surface produces a diffuse angular scattering distribution with an additional broad peak near the specular angle. The degree of specularity increases with increasing incident beam energy or increasing crystal temperature.

The time-of-flight distributions observed at 7° from the surface normal approximate the shape of the Maxwell-Boltzmann distribution for the corresponding crystal temperature. At the specular angle the TOF distributions are generally narrower and shifted in energy from the corresponding Maxwell-Boltzmann distribution, the shift being more evident for high incident beam energy, low crystal temperature, and for low incident beam energy, high crystal temperature. The scattered NO translational energy, as determined as a function of crystal temperature, clearly shows these trends for the specular scattering, and shows deviations from full accommodation for scattering near the surface normal.

The velocity and angular distributions of the sattered NO beam can be

qualitatively discussed in terms of three general scattering mechanisms [1,17]: elastic, inelastic, and trapping desorption. The classification of the scattering behavior is made according to the strength of interaction with the surface. Scattering in which the molecule is in the region of the surface for a long time, relative to a vibrational period, is classified as trapping desorption. Such scattering is characterized by angular distributions which are diffuse and often cosine, and by velocity distributions which are independent of the incident energy, often Maxwell-Boltzmann at the surface temperature.

Scattering in which the molecule experiences a rapid change in normal momentum, what has been called direct scattering [5], and in which there is measurable energy exchange, is classified as inelastic scattering. Direct inelastic scattering generally has narrow angular distributions centered near the specular angle and velocity distributions which are incident energy dependent but only weakly surface temperature dependent.

In cases where there are broad, relatively weak specular scattering or lack of equilibration for apparent trapping desorption scattering, there is a theoretical mechanism which may be important but which would be difficult to confirm experimentally. Theoretical trajectory calculations [18] have suggested that roughness of the surface potential can deflect incident molecules into trajectories along the surface allowing the molecules to slowly transfer momentum and energy to the surface leading the long term trapping. If molecules are deflected again into the gas phase within a short time of the incident collision, they retain memory of their incident energy and, to some extent, direction. One could expect that such scattering would have more energy exchange with the surface and a broader angular distribution than direct inelastic scattering.

Following the definition used in many theoretical papers we define inelastic scattering to be only direct scattering and classify scattering by multiple deflection to be trapping-desorption scattering or short-time trapping desorption scattering when it is necessary to make a distinction.

With the strong interaction potential between NO and the Pt(111) surface, and with exchange of tanslational energy to NO internal energy [10], elastic scattering is only a negligible fraction of the total scattering.

Associating the diffuse portion of the angular distributions with trapping-desorption scattering we see that trapping-desorption is the predominant scattering mechanism. This is consistent with modulated molecular beam kinetic studies [11,12] that found coverage dependent NO sticking probabilities for Pt(111) of approximately .70 to .85 at low coverages.

The broad angular width of the specular peak makes separation of the two components inaccurate; however, we can estimate that the diffuse fraction contributes about 90% of the total scattering in the most diffuse case (Fig.11a) to 80% of the total scattering in the most specular case (Fig.9). The specular peak could originate from broad angle inelastic scattering or possible short time trapping-desorption scattering as defined above, or a combination of the two.

The degree of specularity increases with increasing incident beam energy (Figs. 9c, 10c, 11b) due to the additional energy transfer required for trapping. This indicates that if there is any activation energy barrier to adsorption, it must be less than 0.6 Kcal/mole, our lowest beam energy. The degree of specularity increases with increasing crystal temperature (Fig.9).

To determine whether this effect is due to decreasing roughness from decreasing NO surface coverage, we measured the angular distributions as a function of crystal temperature of the scattered He present in the He seeded NO beam.

From T_s=475 K to T_s=850 K the intensity of the peak in the scattered He angular distribution increased with crystal temperature due to decreasing NO coverage. Above 850 K the scattered He intensity declined with increasing temperature due to increasing thermal disorder of the platinum. In contrast the NO specular peak shows a monotonic increase in intensity. The increased specularity with increasing surface temperature is primarily due to a temperature dependence in the trapping probability as seen for N_2 on W [4] and Ar on W [6].

From the angular distributions we anticipate that there will be two contributions to the time-of-flight distributions, the more accommodated molecules from trapping desorption and the molecules in the specular peak which are from inelastic and/or incompletely accommodated scattering. From angular measurements we have concluded that we can observe predominantly accommodated trapping-desorption scattering only near the surface normal and only for low crystal temperature and incident beam energy, and that there is no condition under which we can observe predominantly specular scattering behavior. In general, the TOF distributions will be a sum of two distributions, the average energy will be the average of the separate average energies, the width, $\langle\sigma^2\rangle$ will be determined by the individual widths, and the separation of the average energies.

A search by varying detector angles and incident angles and crystal temperature failed to produce any conditions under which the two scattering mechanisms are distinguishable or separable in the TOF distributions. In this respect, NO scattering from Pt(111) is similar to N_2 from W [4], and Ar from W [6], and unlike Xe from Pt(111) [5], for which a bimodal velocity distributon was observed.

With the above considerations, the trends in average energy and width, $\langle\sigma^2\rangle$,

of the TOF distribtions of the scattered NO can be readily explained. For the 1390 K incident beam (Fig.6), the equivalent temperature of the scattered beam is higher than the surface temperature from T_s=475 K to T_s=900 K, with less accommodation for molecules scattered at specular than for those scattered at 7° from the surface normal. From T_s=900 K to T_s=1195 K, the equivalent temperature is nearly equal to the surface temperature. From the energy one might conclude that the scattered molecules are equilibrated with the surface. The width, $\langle\sigma^2\rangle$, (Fig.6b) of the distribution for molecules scattered near 7° is near .13, the value for a Maxwell-Boltzmann distribution, but $\langle\sigma^2\rangle$ for the distribution for scattering at the specular angle is much narrower. Thus moleucles scattered near the specular angle are clearly not equilibrated. The width of the specularly scattered distribution increases with decreasing temperature due to the increasing separation in energy between the accommodated molecules and inelastically scattered and incompletely accommodated molecules. At T_s=1195 K the average scattered energy appears to be less than the incident energy and crystal temperature. This is probably due to transfer of translational energy to initially cool NO rotational modes as has been observed on Ag [10].

It can be seen that the degree of accommodation is greater for scattering 7° from the surface normal than for scattering at the specular angle which is expected due to the greater contribution from inelastic scattering near specular. However, for scattering near the surface normal, T_s=475 K (Fig. 6b) the lack of accommodation is unusual given the weakness of specular feature in the angular distribution (Fig.9a). From this we conclude that the inelastic scattering has as extremely broad angular distribution, or that there might be significant contribution from short-time trapping-desorption scattering.

At lower incident beam energies, T_B=615 K (Fig.7), the scattered beam equivalent temperature is equal to the surface temperature up to Ts=725 K,

then becomes increasingly lower than T_S with increasing temperature. From the width of the distributions (Fig. 7b), it can be seen that at lower crystal temperatures the molecules scattered near the surface normal are essentially equilibrated with the crystal, but the time-of-flight distributions of molecules scattered at the specular angle are too narrow for equilibrated scattering. This is again due to the greater contribution of inelastic scattering at the specular angle.

For the 265 K equivalent temperature incident beam, the scattered energies (Fig.8) show the same trends as observed with T_B=615 K. The lack of equilibration for scattering at 7° and T_S>900 K is pronounced for T_B=265 K and T_B=615 K. Since the probability of trapping, as evidenced in the degree of specularity and in the velocity distributions, decreases with increasing beam energy, by detailed balance arguments there must be a deficiency in the high energy part of the desorption flux. Therefore, the lack of equilibration may be partially due to non-equilibrated desorption. However, the degree of accommodation for scattering near the surface normal at T_S=1000 K and T_S=1195 K is lower for T_B=265 K than for T_B=615 K incident beam, so there is significant contribution from inelastic scattering and incompletely accommodated molecules.

Acknowledgements

This work was supported by the Director, Office of Energy Research, Office of Basic Energy Sciences, Materials Sciences Division of the U.S. Department of Energy under Contract W-7405-ENG-48, and the National Science Foundation.

We would like to thank Dr. M. Asscher for his help, and Professor G. Ertl for many discussions.

References

1. W.H. Weinberg, Adv. in Colloid & Interface Science, 4 (1975) 301.

2. S.T. Ceyer and G.A. Somorjai, Ann. Rev. Phys. Chem. 28 (1977) 477.

3. J. Lapujoulade and Y. Lejay, J. Chem. Phys. 63 (1975) 1389.

4. K.C. Janda, J.E. Hurst, C.A. Becker, J.P. Cowin, L. Wharton, and D.J. Auerbach, Surface Sci. 93 (1980) 270.

5. J.E. Hurst, C.A. Becker, J.P. Cowin, K.C. Janda, L. Wharton, and D.J Auerbach, Phys. Rev. Lett. 43 (1979) 1175.

6. K.C. Janda, J.E. Hurst, C.A. Becker, J.P. Cowin, D.J. Auerbach, and L. Wharton, J. Chem. Phys. 72 (1980) 2403.

7. J.R. Arthur and T.R. Brown, J. Vac. Sci. Technol. 12 (1975) 200.

8. F. Frenkel, J. Hager, W. Krieger, H Walther, C.T. Campbell, G. Ertl, H. Kuipers, and J. Segner, Phys. Rev. Lett. 46 (1981) 152.

9. G.M. McClelland, G.D. Kubiak, H.G. Rennagel, and R.N. Zare, Phys. Rev. Lett. 46 (1981) 831.

10. A.W. Kleyn, A.C. Luntz, and D.J. Auerbach, private communication, 1981.

11. T.-H. Lin and G.A. Somorjai, Surface Sci. 107 (1981) 573.

12. C.T. Campbell, G. Ertl, and J. Segner, private communication.

13. S.T. Ceyer, W.J. Siekhaus, and G.A. Somorjai, in press.

14. S.T. Ceyer, Ph.D. Thesis, University of California, Berkeley, 1979.

15. C.T. Campbell and G. Ertl, private communication.

16. H. Saltsburg, An. Rev. Phys. Chem. 24 (1973) 493.

17. R. Sau and R.P. Merrill, Surface Sci. 34 (1973) 268.

Figure Captions

1. Schematic diagram of molecular beam scattering apparatus.

2. Time-of-flight distribution for direct nozzle beam with beam energy $\langle KE \rangle/2k=1390$ K.

3. Time-of-flight distribution for an effusive 300 K direct NO beam. The solid curve is the Maxwellian distribution at 300 K.

4. Time-of-flight distributions for (a) $T_B=615$ K, TS=475 K; detector sits at 7° from normal, (b) $T_B=615$ K, $T_S=475$ K, specular detection. The solid curves are the Maxwsellian distributions at the corresponding surface temperature.

5. Time-of-flight distributions for (a) $T_B=1390$ K, $T_S=475$ K, 7° from normal detection, (b) $T_B=1390$ K, $T_S=1110$ K, specular detection. The solid curves are the Maxwellian distributions at the corresponding surface temperatures

6a. Correlation of $\langle KE \rangle/2k$ of the scattered beam with respect to surface temperature, $T_B=1390$ K.

6b. Correlation of $\langle \sigma^2 \rangle$ of the scattered beam with respect to surface temperature, $T_B=1390$ K. The arrow on the left specifies the value of a Maxwellian distribution.

7a. Correlation of $\langle KE \rangle/2k$ of the scattered beam with respect to surface temperature, TS=615 K.

7b. Correlation of $\langle \sigma^2 \rangle$ of the scattered beam with respect to surface temeprature, $T_B=615$ K. The arrow on the left specifies the value of a Maxwellian distribution.

8. Correlation of $\langle KE \rangle/2k$ of the scattered beam with respect to surface temperature, $T_B=265$ K.

9. Angular distributions for $T_B=1390$ K, (a) Ts=475 K, (b) Ts=725 K, (c) Ts= 1195 K.

10. Angular distributions for $T_B=615$ K, (a) Ts=475 K, (b) Ts=725 K, (c) Ts= 1195 K.

11. Angular distributions for $T_B=265$ K, (a) Ts=725 K, (b) Ts=1195 K.

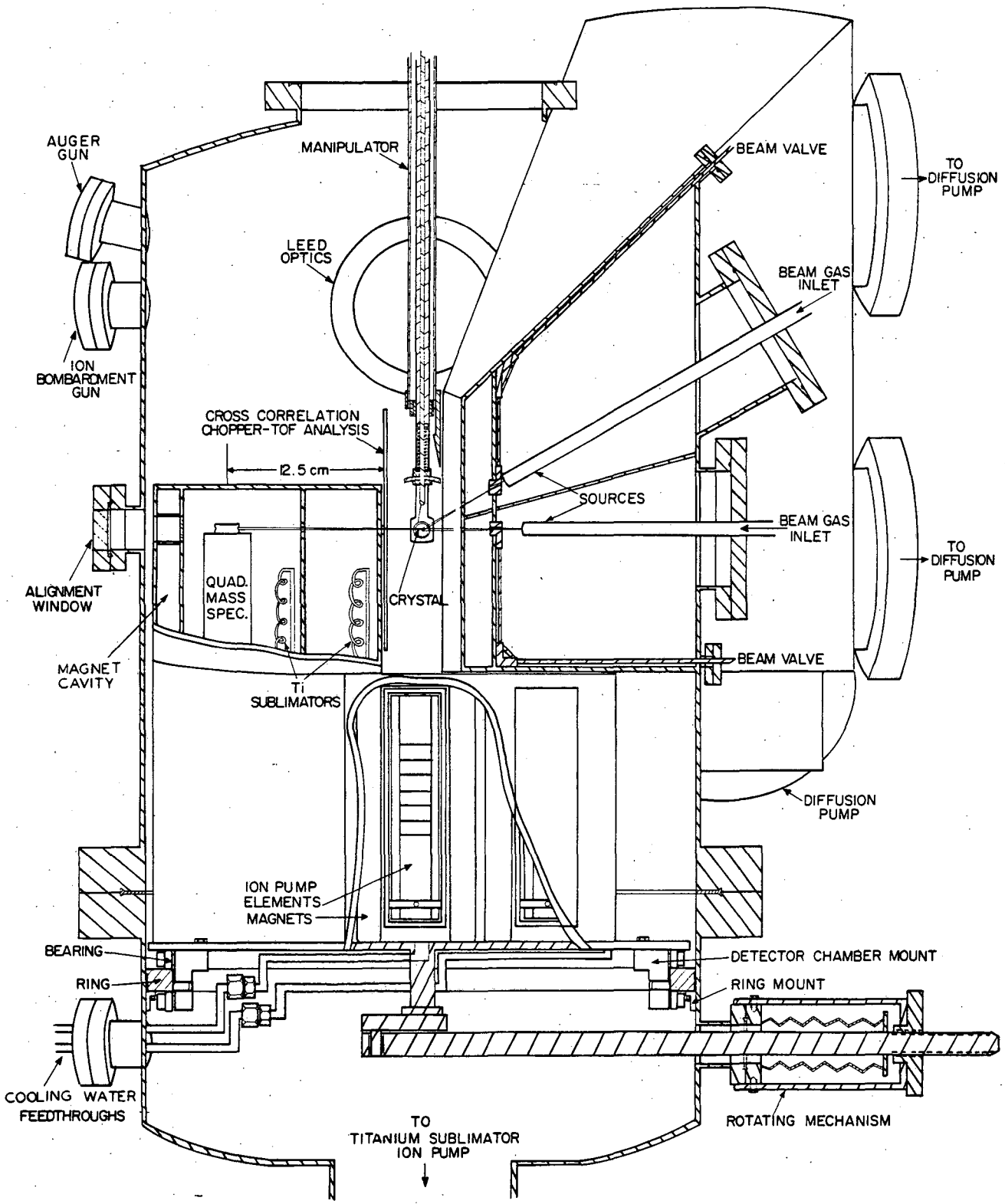

XBL 799-11376

Fig.1

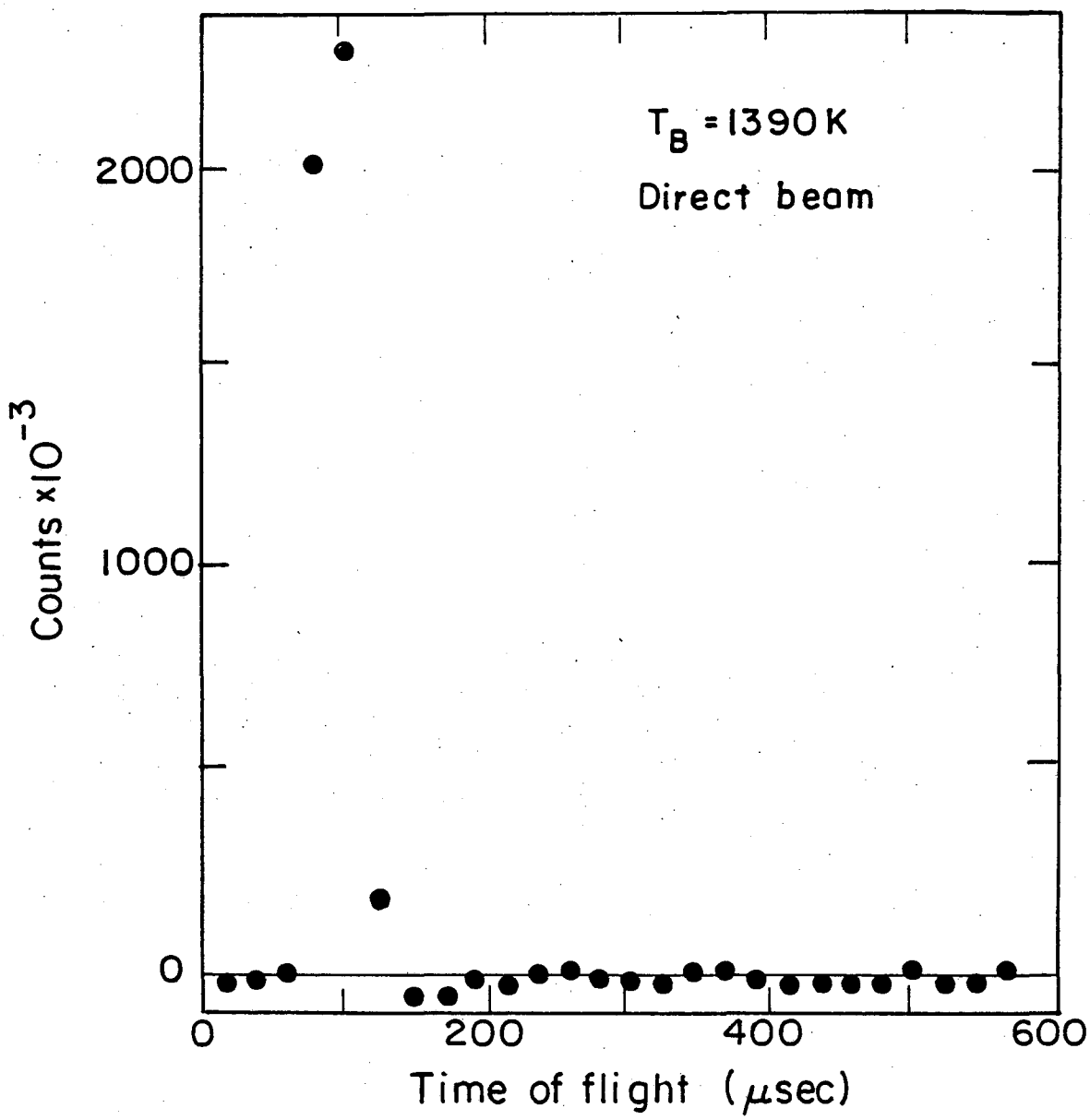

XBL 819-6599

Fig.2

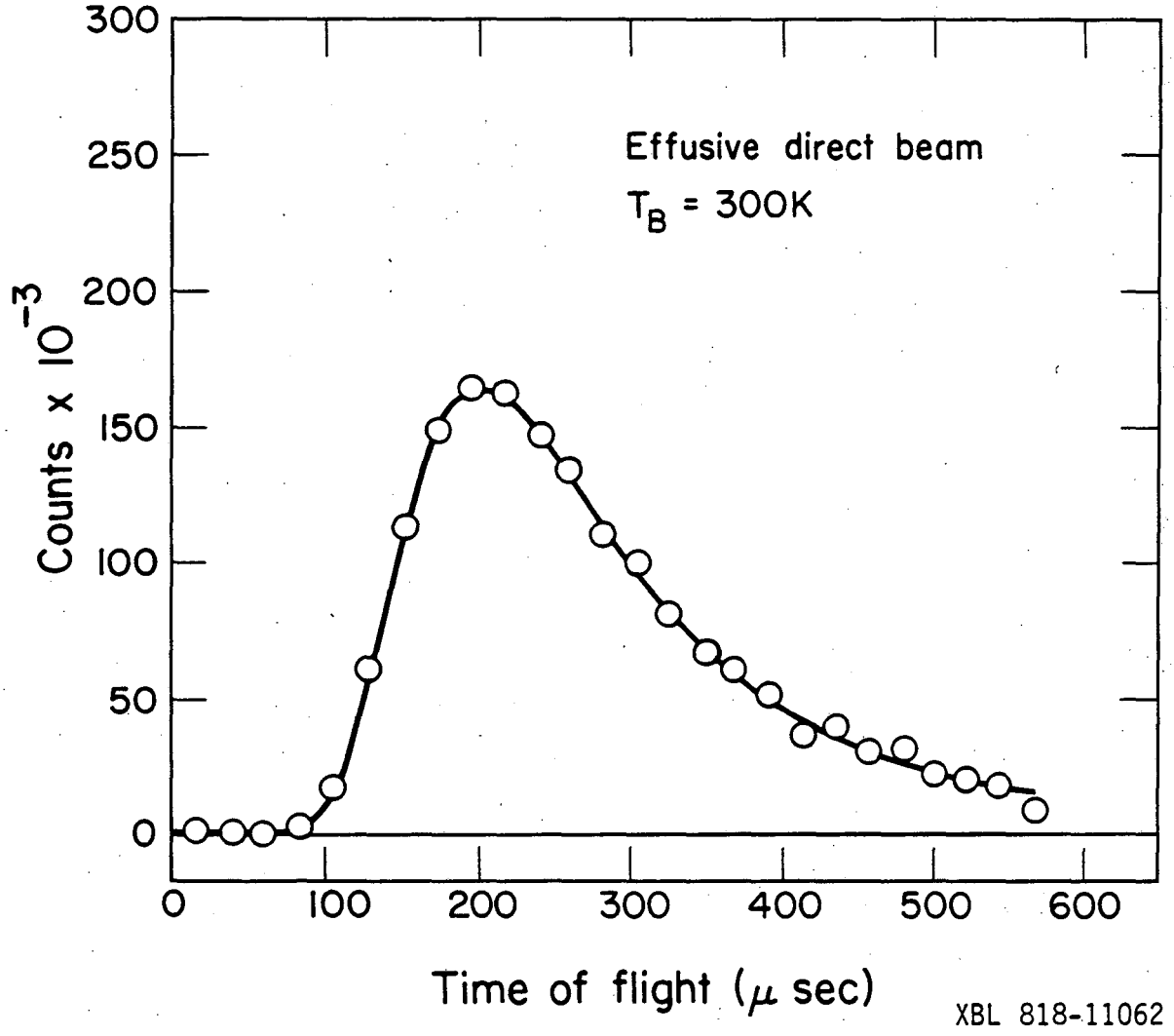

XBL 818-11062

Fig.3

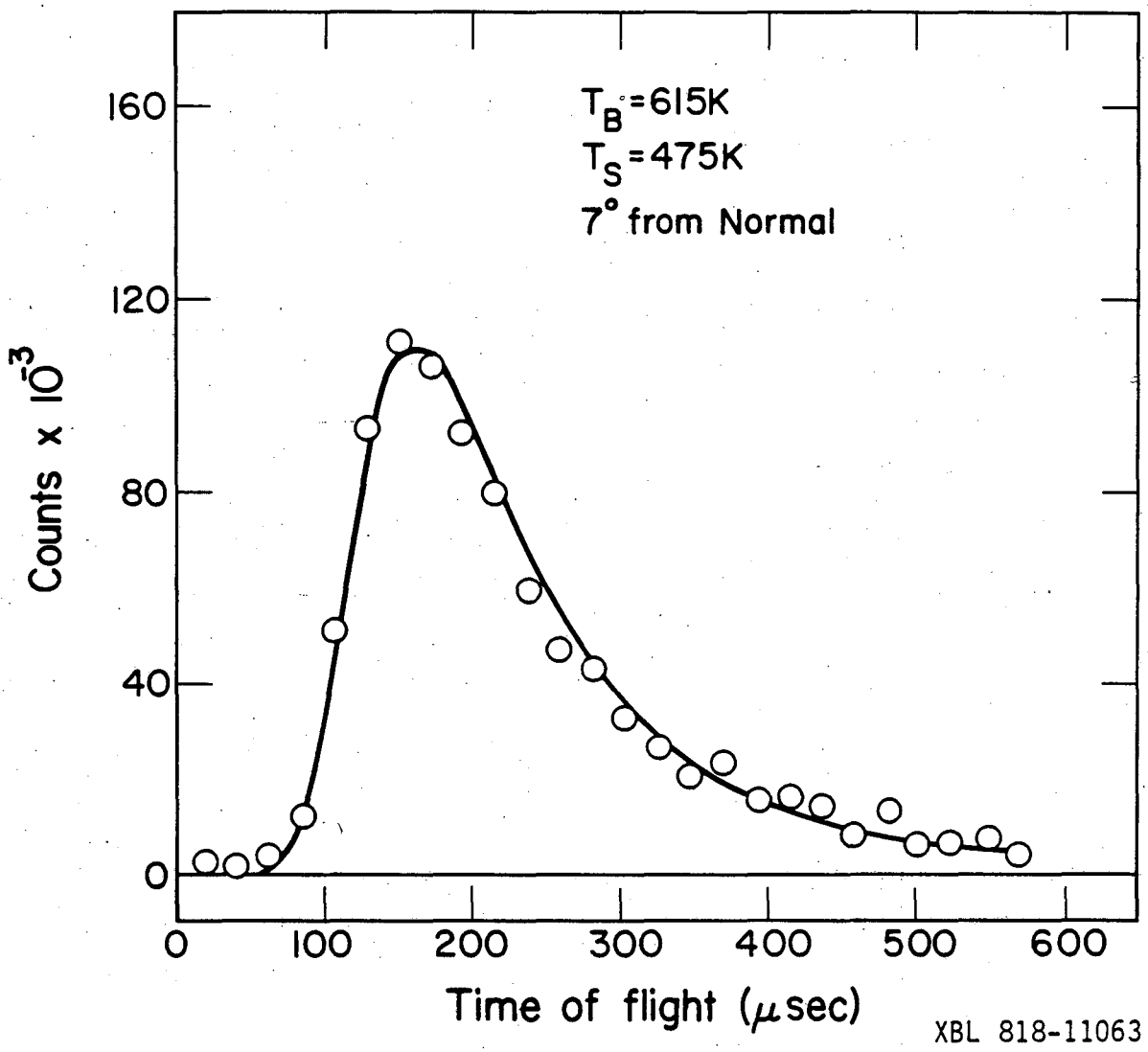
T_B=615K
T_S=475K
7° from Normal
Counts x 10^{-3}
160
120
80
40
0
0
100
200
300
400
500
600
Time of flight (μsec)
XBL 818-11063

Fig.4a

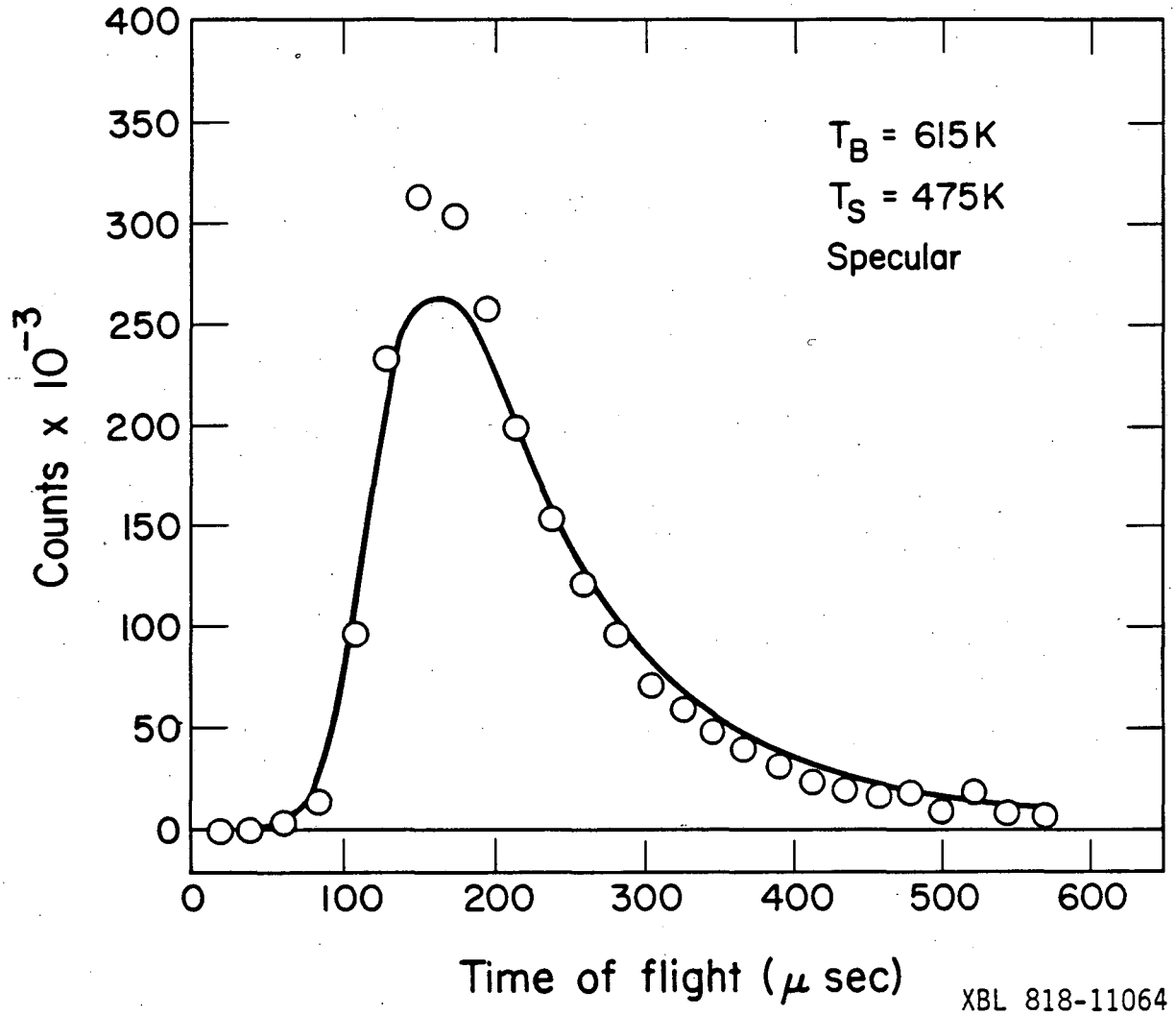

XBL 818-11064

Fig.4b

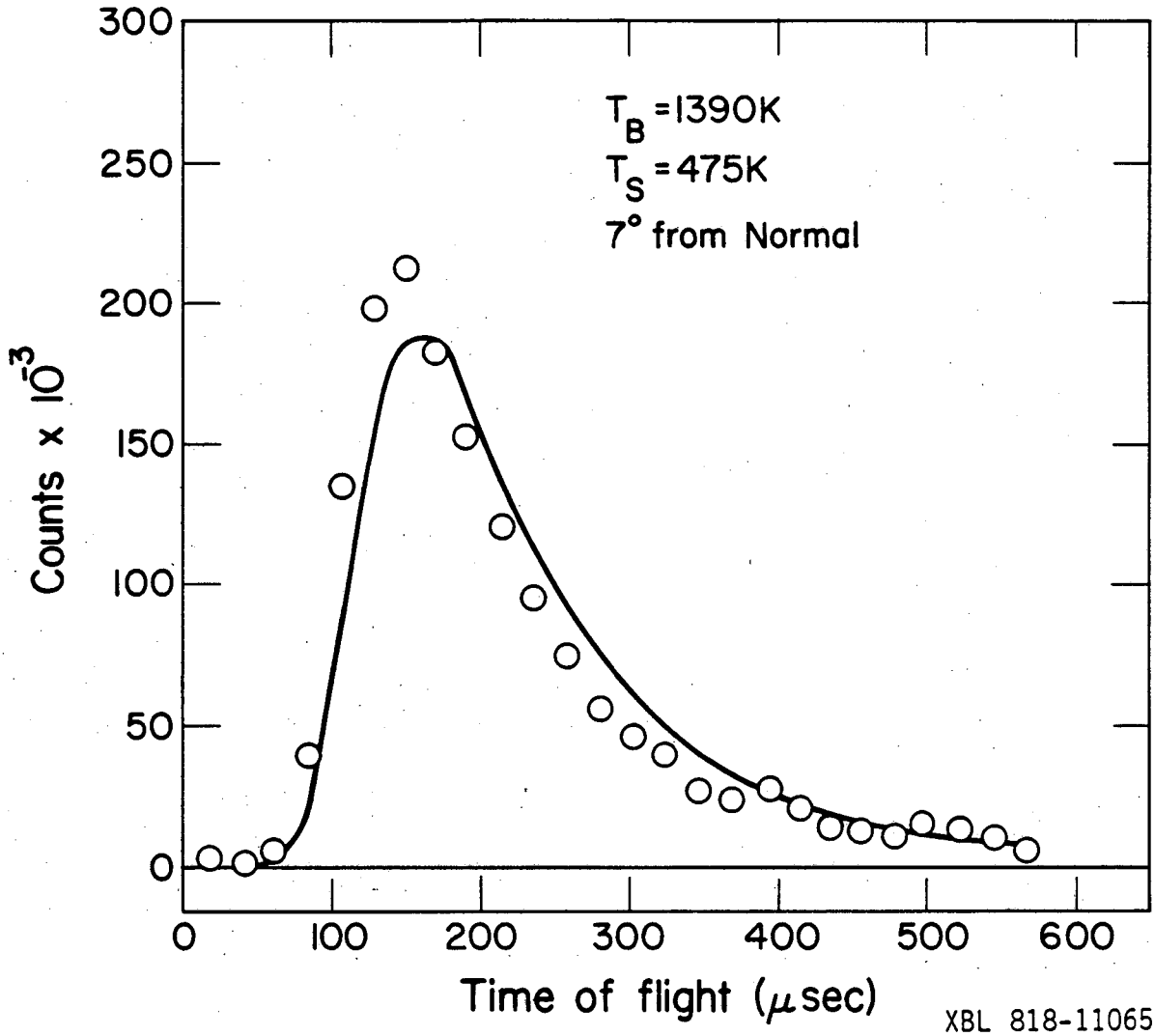
300
250
200
150
100
50
0
Counts x 10^{-3}
T_B =1390K
T_S =475K
7° from Normal
0
100
200
300
400
500
600
Time of flight (μsec)
XBL 818-11065

Fig.5a

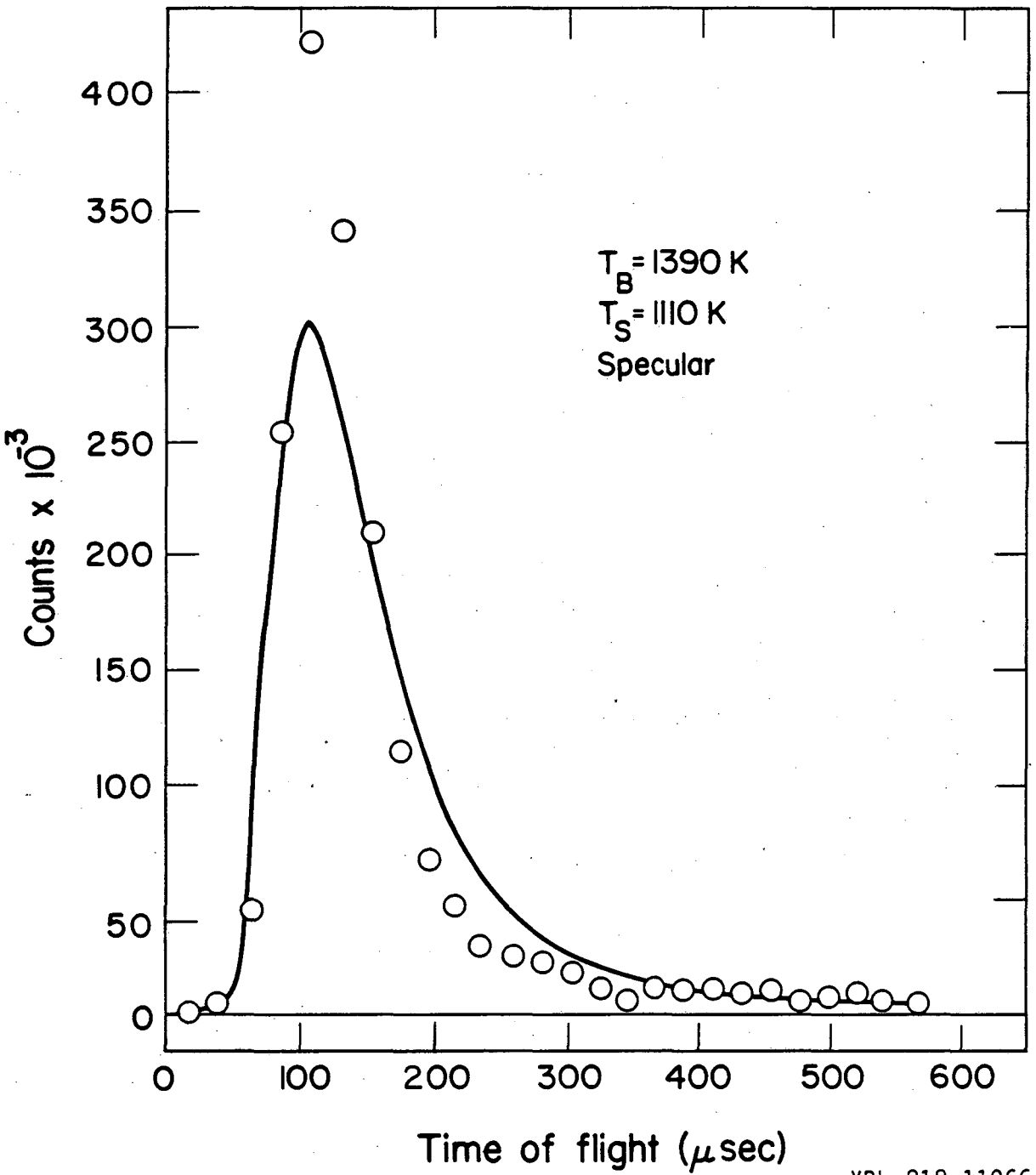

XBL 818-11066

Fig.5b

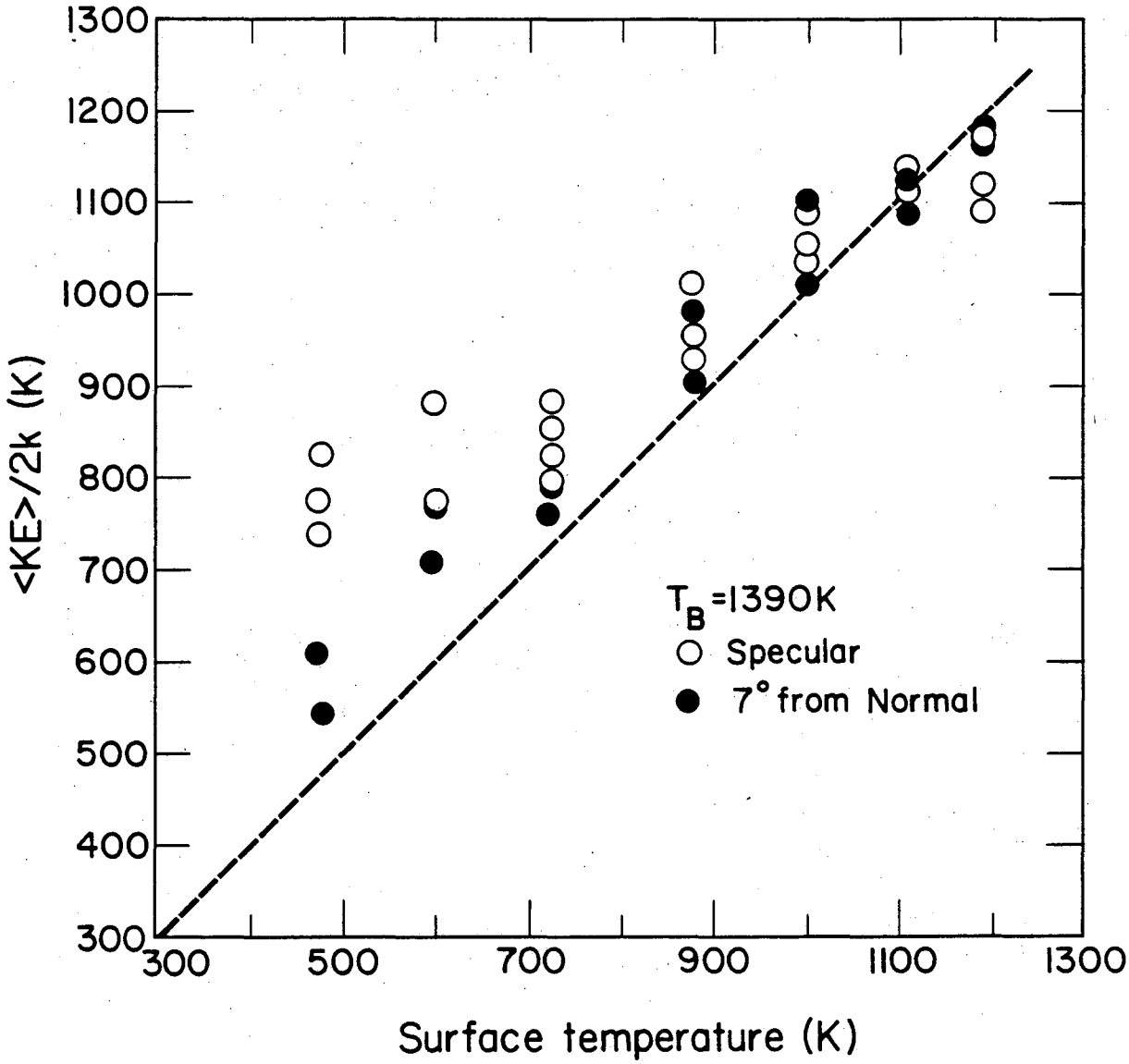

XBL 818-11052

Fig.6a

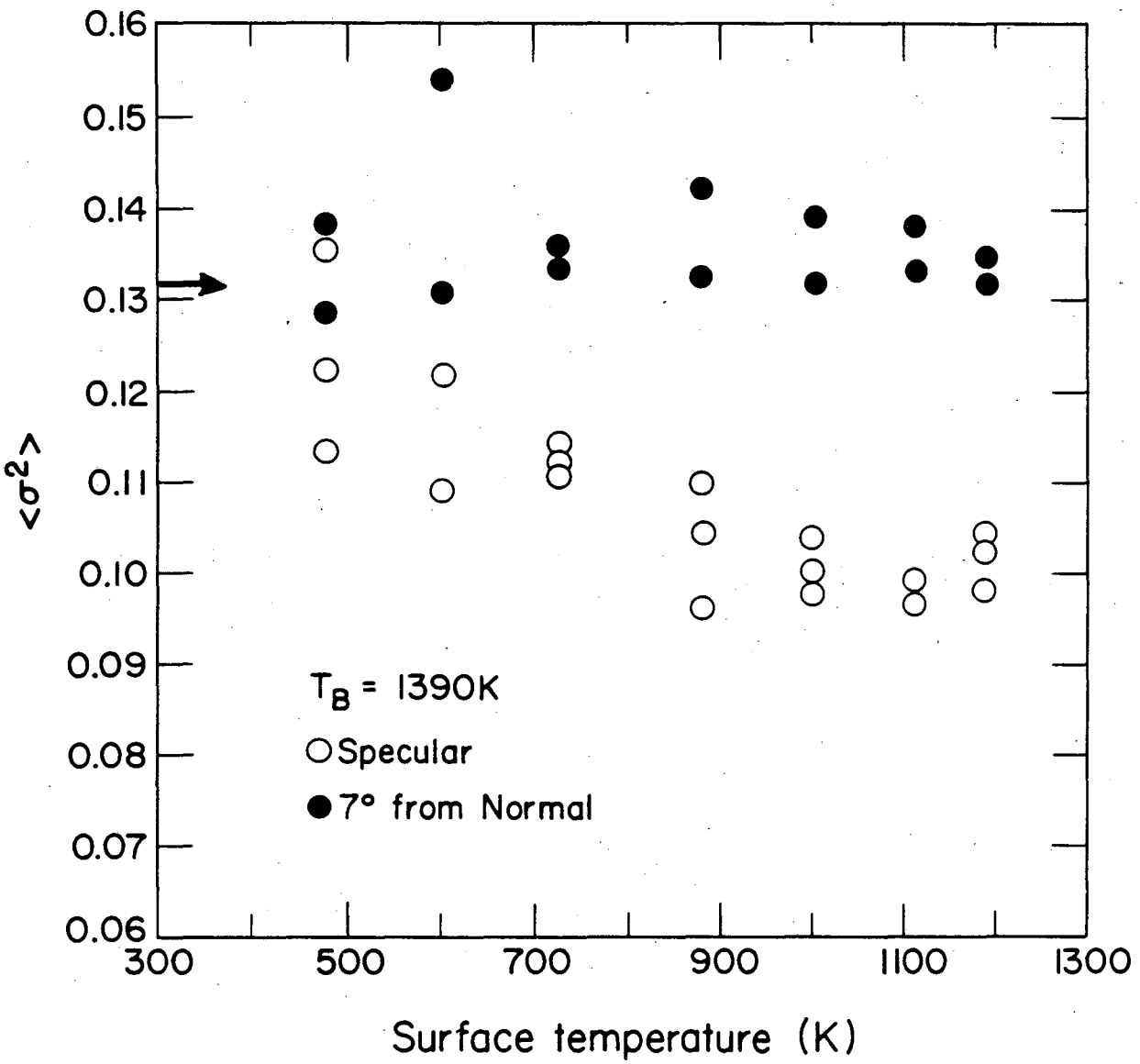

XBL 818-11051

Fig.6b

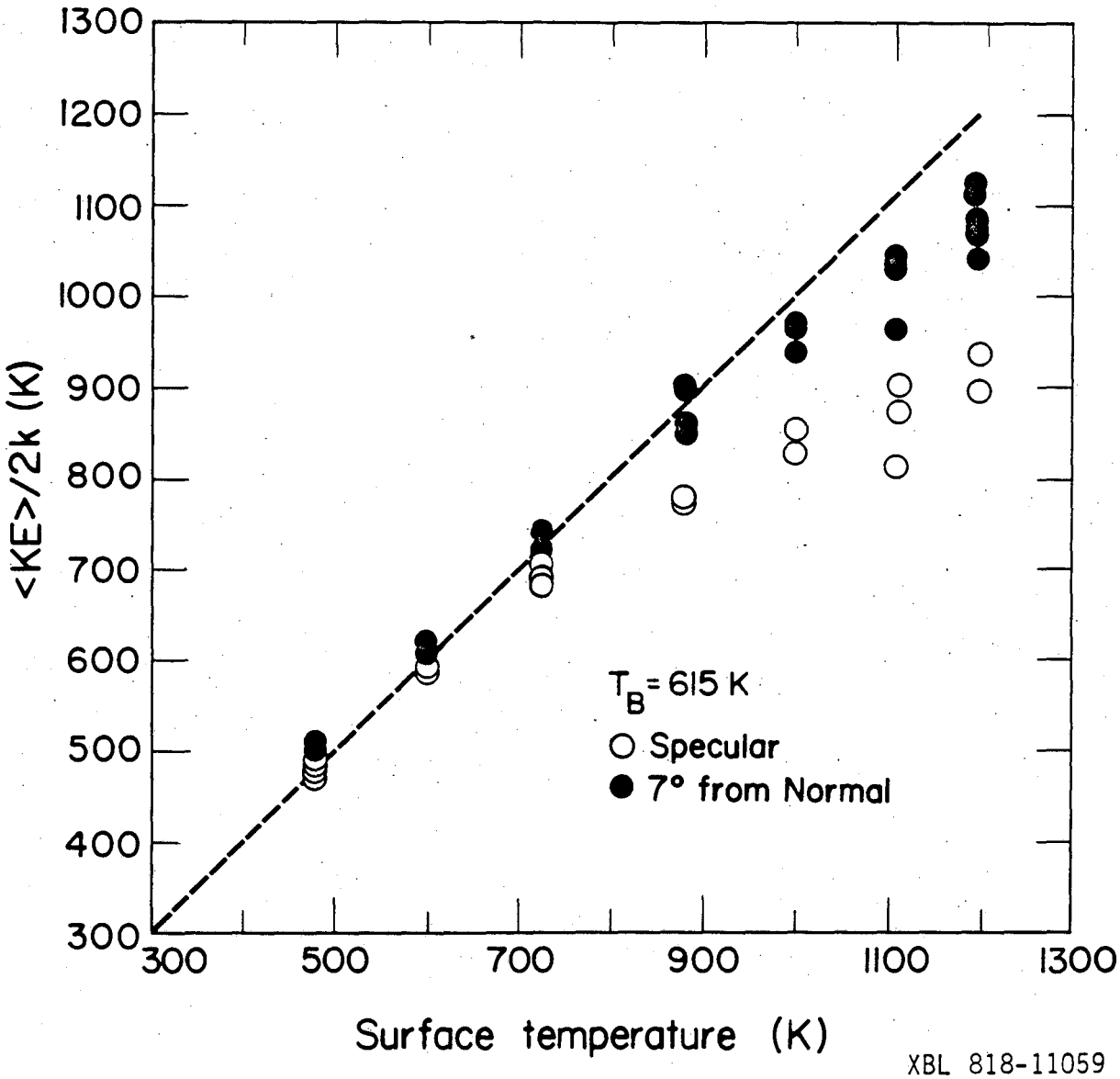
1300
1200
1100
1000
900
800
700
600
500
400
300
<KE>/2k (K)
300
500
700
900
1100
1300
Surface temperature (K)
T_B = 615 K
Specular
7° from Normal
XBL 818-11059

Fig.7a

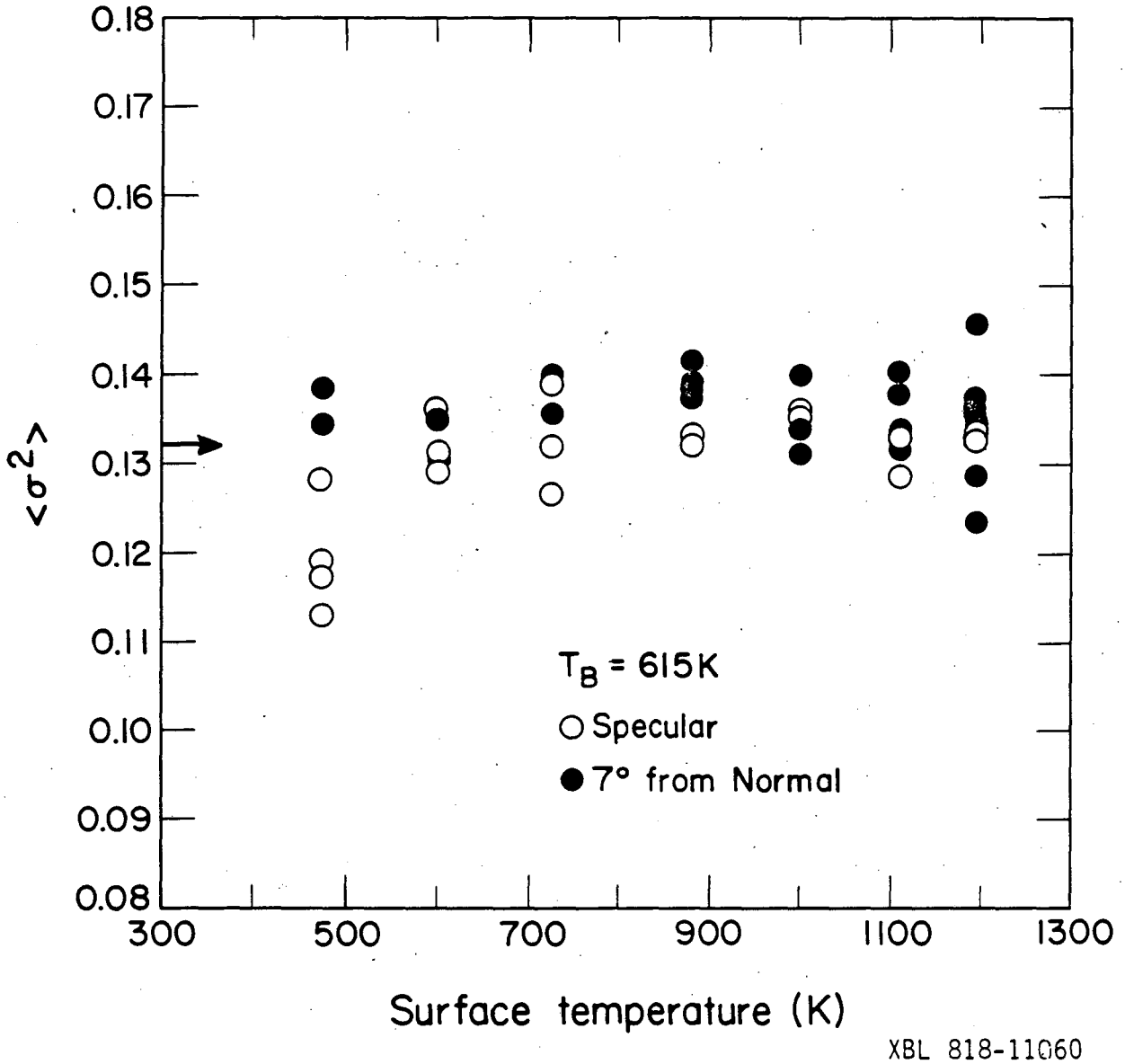
0.18
0.17
0.16
0.15
0.14
0.13
0.12
0.11
0.10
0.09
0.08
<σ²>
300
500
700
900
1100
1300
Surface temperature (K)
T_B = 615K
Specular
7° from Normal
XBL 818-11060

Fig.7b

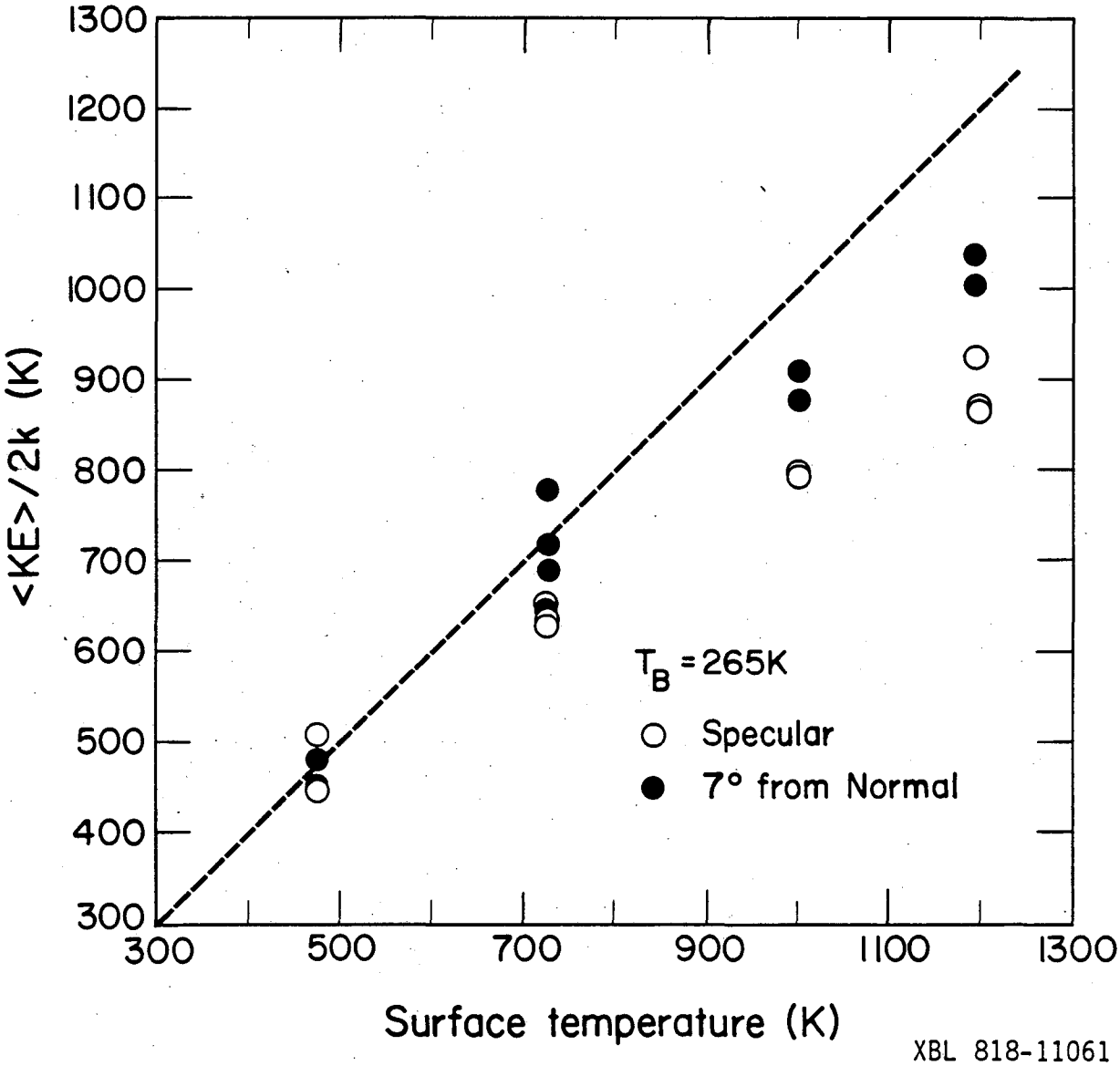
1300
1200
1100
1000
900
800
700
600
500
400
300
<KE>/2k (K)
300
500
700
900
1100
1300
Surface temperature (K)
T_B = 265K
Specular
7° from Normal
XBL 818-11061

Fig. 8

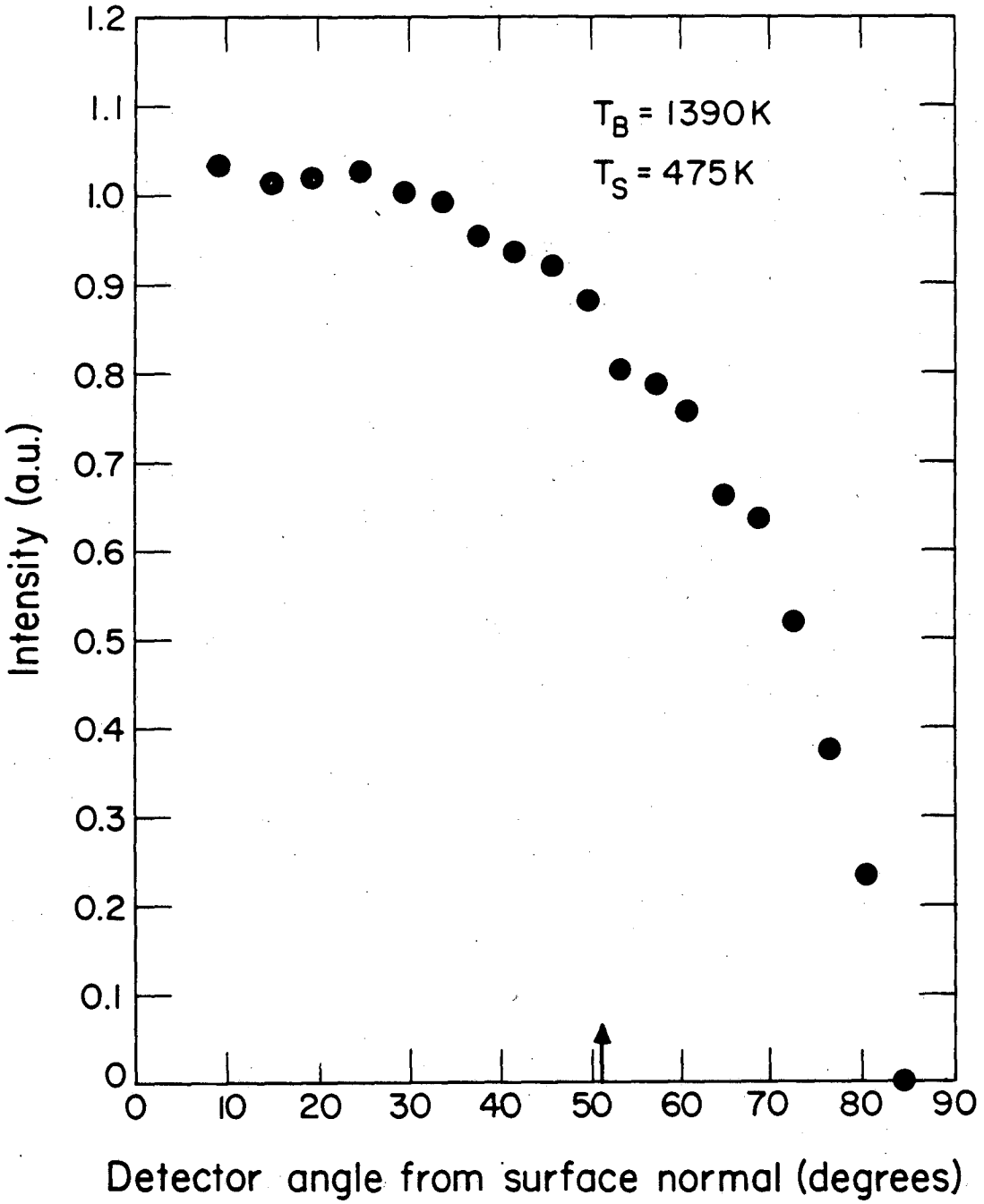

XBL 818-11055

Fig. 9a

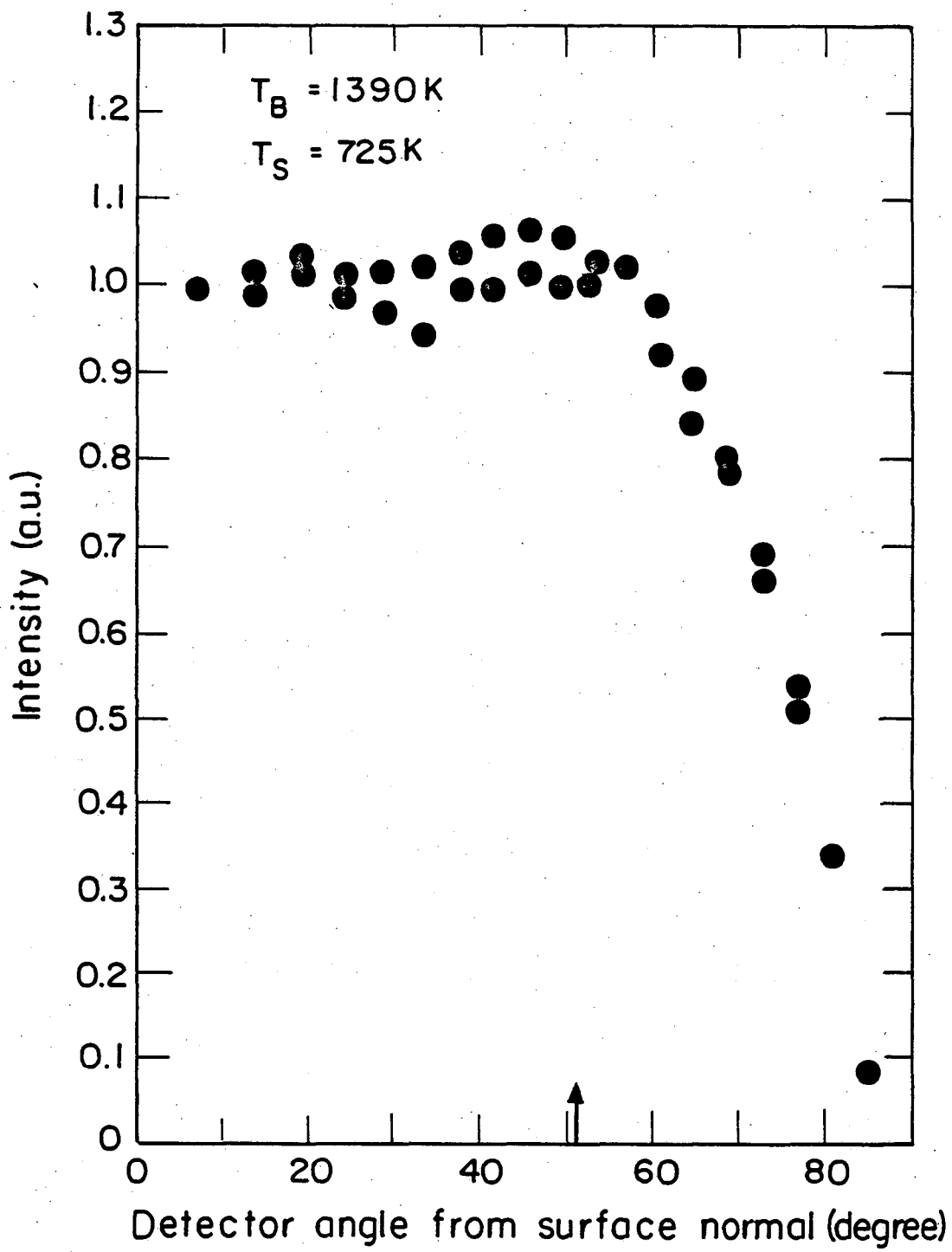

XBL 819-6598

Fig. 9b

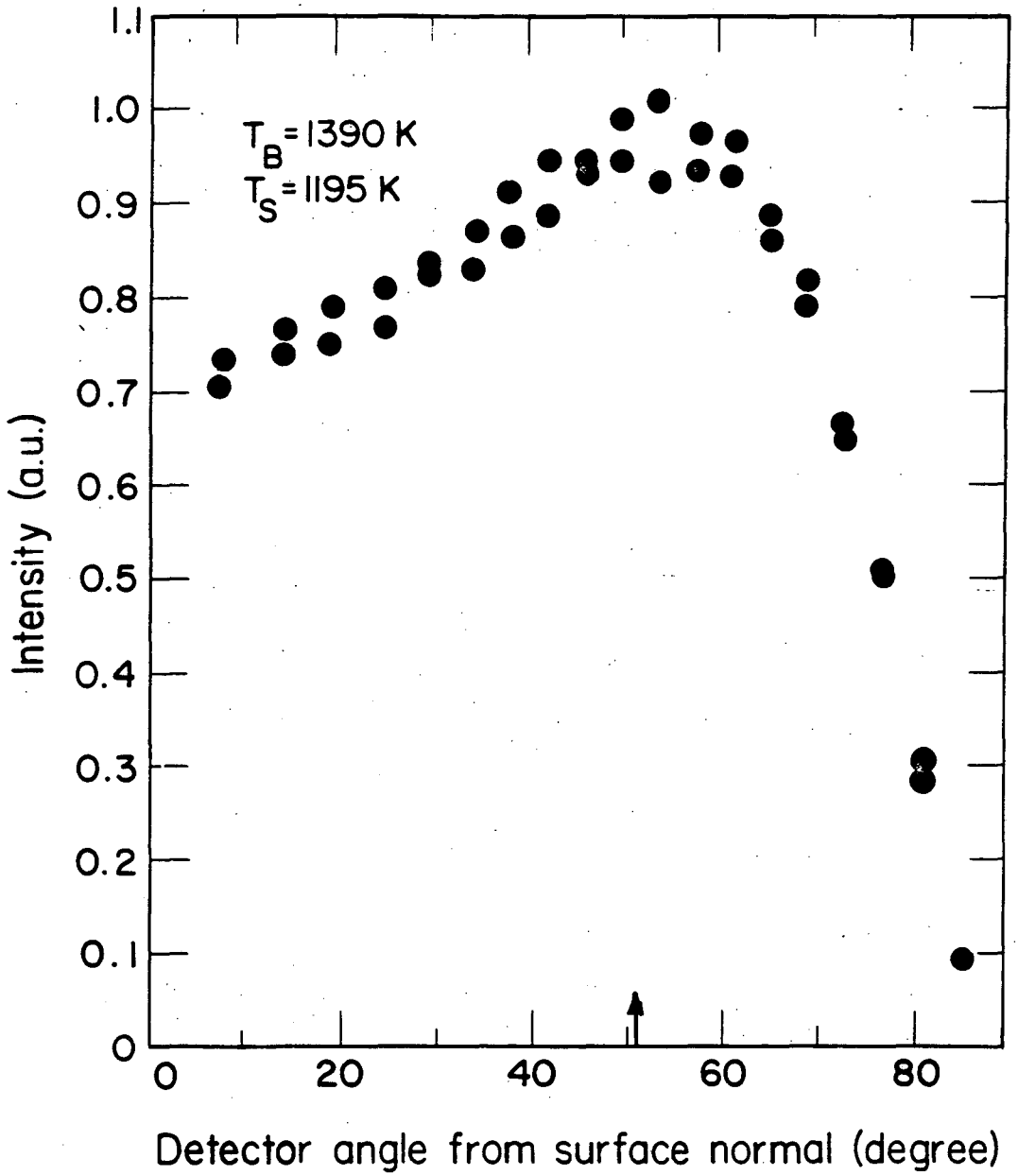

XBL 818-11054

Fig. 9c

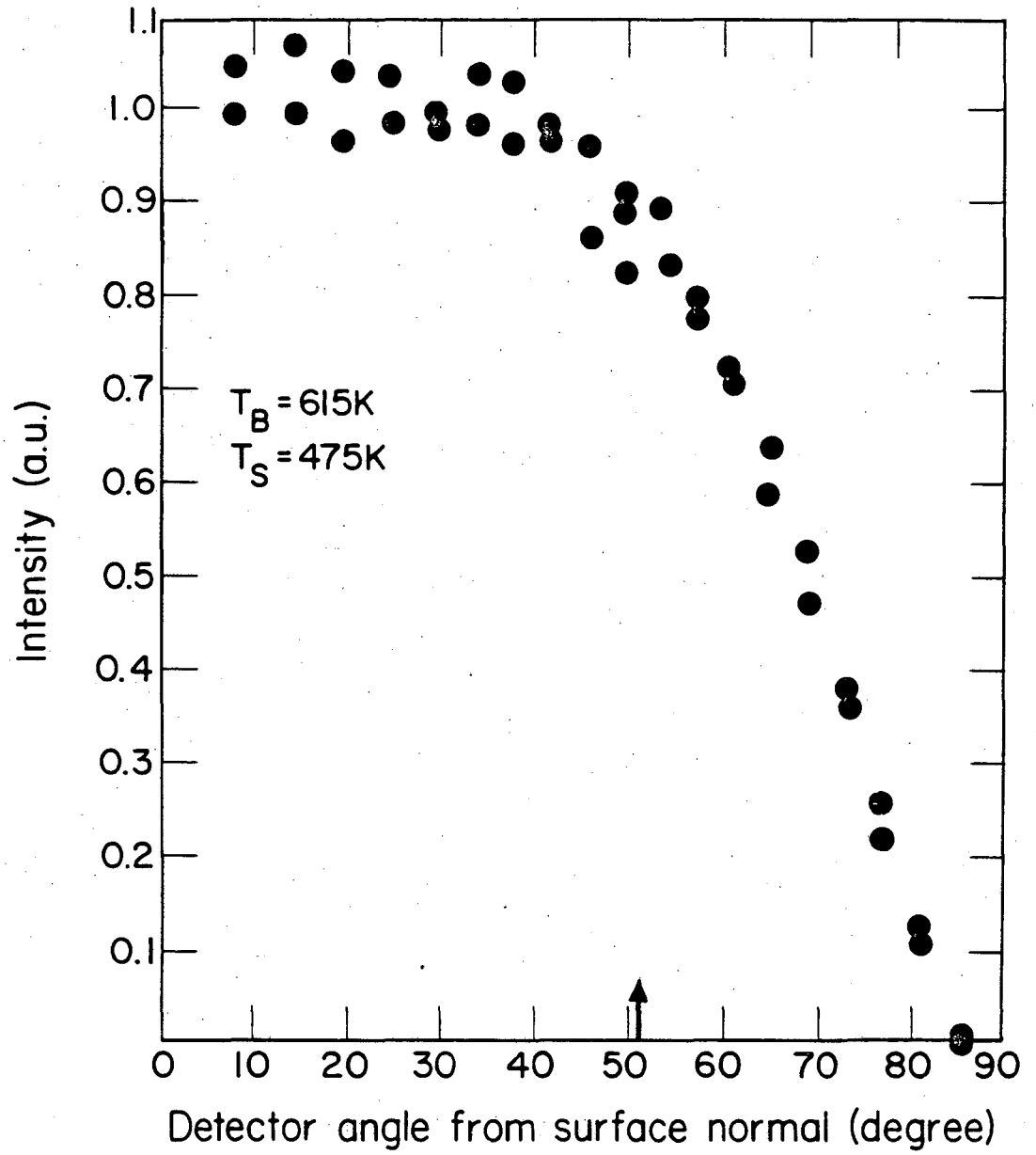

XBL 818-11056

Fig.10a

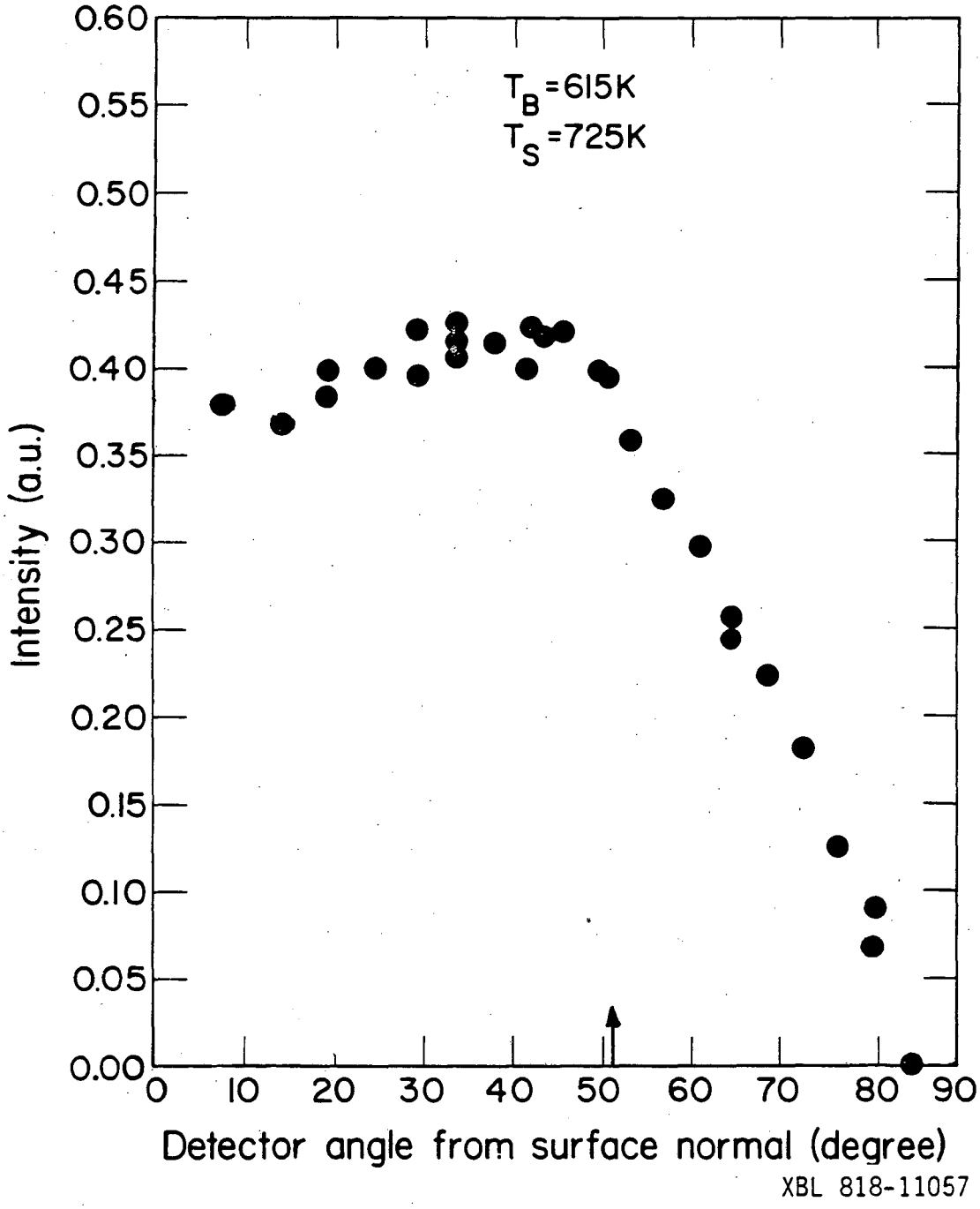
T_B=615K
T_S=725K
Intensity (a.u.)
0.60
0.55
0.50
0.45
0.40
0.35
0.30
0.25
0.20
0.15
0.10
0.05
0.00
0
10
20
30
40
50
60
70
80
90
Detector angle from surface normal (degree)
XBL 818-11057

Fig.10b

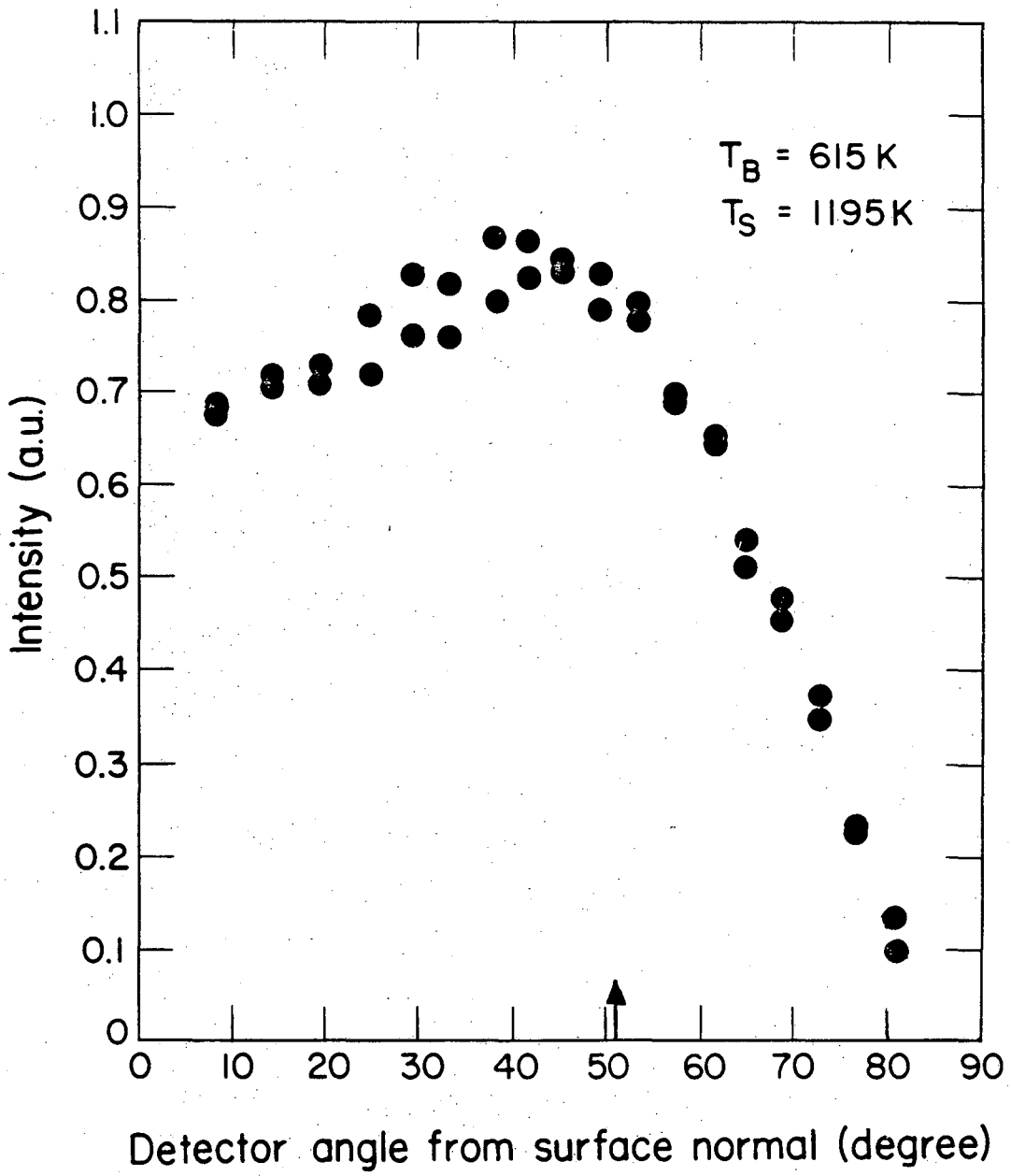

XBL 818-11058

Fig.10c

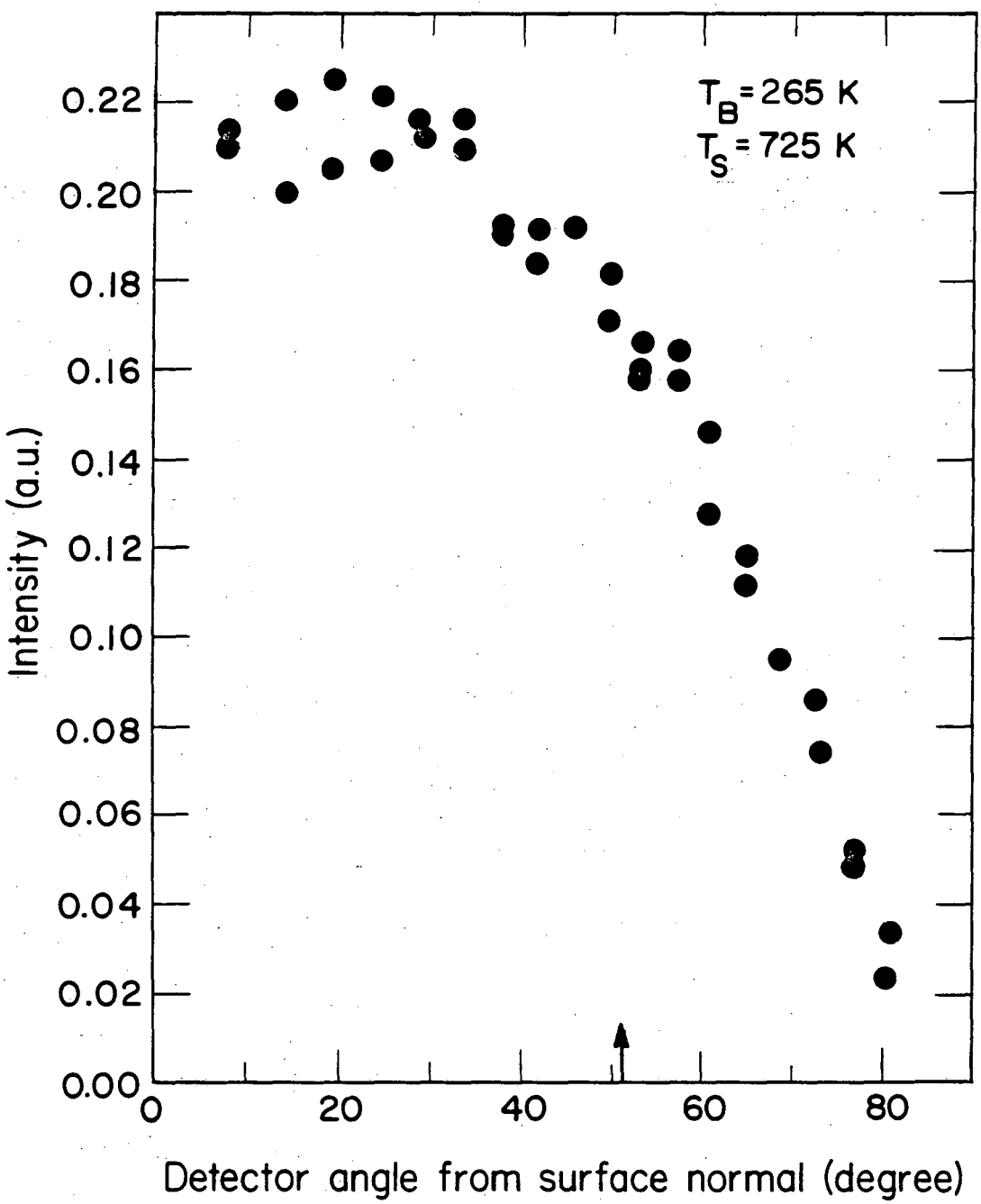

XBL 818-11068

Fig.11a

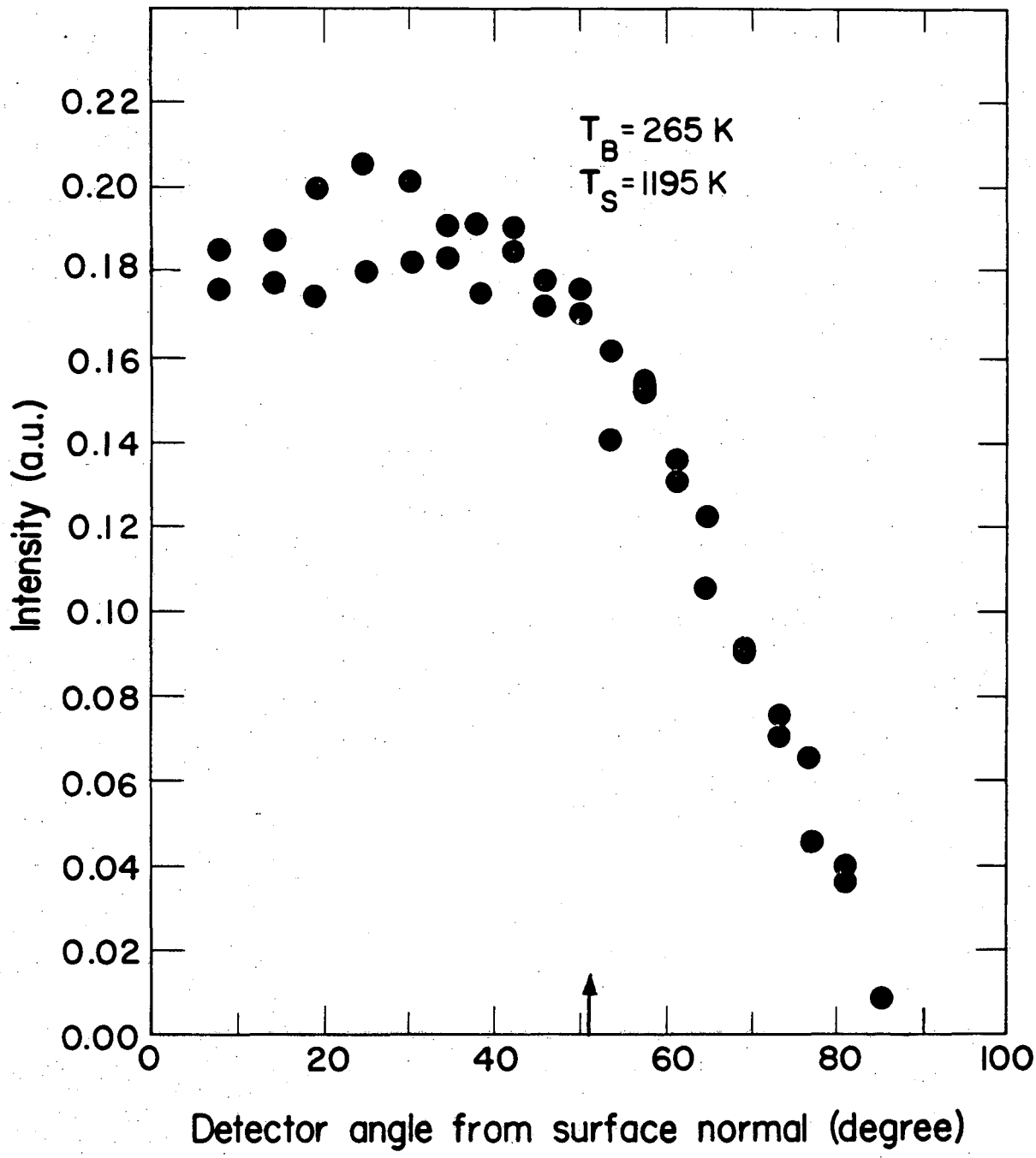

XBL 818-11067

Fig.11b

This report was done with support from the Department of Energy. Any conclusions or opinions expressed in this report represent solely those of the author(s) and not necessarily those of The Regents of the University of California, the Lawrence Berkeley Laboratory or the Department of Energy.

Reference to a company or product name does not imply approval or recommendation of the product by the University of California or the U.S. Department of Energy to the exclusion of others that may be suitable.

TECHNICAL INFORMATION DEPARTMENT
LAWRENCE BERKELEY LABORATORY
UNIVERSITY OF CALIFORNIA
BERKELEY, CALIFORNIA 94720